Paper pa01-088
Submitted to the 28th International Conference on High Energy Physics
ICHEP'96, Warsaw, Poland, July 1996

Elastic ϱ' Electroproduction at High Q^2

H1 Collaboration

Abstract

In data collected in 1994 by the H1 detector at HERA, corresponding to a luminosity of 1.96 pb^{-1}, a significant enhancement is reported in the $\pi^+\pi^-\pi^+\pi^-$ invariant mass spectrum of the elastic electroproduction reaction $ep \rightarrow e\pi^+\pi^-\pi^+\pi^- p$. The signal can be interpreted in terms of the production of a single resonance with mass 1.57 ± 0.02 GeV/c^2 and width 0.18 $\pm$ 0.09 GeV/c^2. It can also be analysed in terms of interfering production of the vector meson resonances $\varrho'(1450)$ and $\varrho'(1700)$. Significant $\varrho(770)$ production is observed in the decay products. The t dependence of the signal indicates peripheral production. The ratio of the cross sections $ep \rightarrow ep\varrho'(\pi^+\pi^-\pi^+\pi^-)$ to $ep \rightarrow ep\varrho$, for the kinematic range $4 < Q^2 \lesssim 50$ GeV^2, $40 < W < 140$ GeV/c^2 is measured to be $0.36 \pm 0.07 \pm 0.11$, significantly higher than at low Q^2.

1 Introduction

This paper is concerned with the study of the elastic reaction

$$ep \rightarrow e\pi^+\pi^-\pi^+\pi^- p \tag{1}$$

for high photon virtuality, using the H1 detector at the HERA ep collider at DESY in Hamburg.

A strong enhancement is observed in the $\pi^+\pi^-\pi^+\pi^-$ invariant mass $m_{4\pi}$ at ~ 1.55 GeV/c^2, a value close to that attributed in previous experiments to the $\varrho'(1600)$ resonance. The interpretation of $\varrho'(1600)$ as a single resonance has been questioned, and an alternative analysis of the existing data as due to two interfering resonances has been proposed (see review in [1]). After a presentation of the experimental conditions in sections 2–4, the nature of the signal in this experiment is discussed in section 5.

The present study is carried at much higher energy than previous experiments: W, the invariant mass of the hadron system, is in the range $40 < W < 140$ GeV/c^2, while it did not exceed $\simeq 12$ GeV/c^2 in the past (the highest energy experiments are [2, 3, 4] [1]). The elastic production and decay of the meson resonances are thus not complicated in the present case by kinematic reflections, for example due to baryon resonance production.

Very significant is also the high virtuality of the exchanged photon reached in this experiment: the range in Q^2, the negative of the four–momentum squared of the photon, is $4 < Q^2 \lesssim 50$ GeV^2, while it was $\lesssim 1$ GeV^2 for previous leptoproduction experiments [4, 6].

The production characteristics of the signal are discussed in section 6.

A striking feature of the present data is the significant increase of the cross section ratio for ϱ' [2] and ϱ meson elastic production, compared to low Q^2 results (see section 6.3). Such an evolution has been predicted in a QCD framework [7]. With increasing Q^2, the transverse size of the $q\bar{q}$ pair (colour dipole) coupling to the virtual photon shrinks to smaller values. The convolution of the dipole transverse extension with the final state vector meson wave function, through the dipole–proton cross section, leads to a "scanning" with Q^2 of the vector meson transverse size, following the expression of [8]. Predictions for the effect given in [9, 10] are briefly discussed.

The present data is thus a first step in detailed studies of this important effect, directly related to the understanding of the nature of diffraction and of the pomeron.

2 Detector and Event Selection

The data used correspond to a total integrated luminosity of 1.96 pb^{-1} collected in 1994. During this data taking period HERA operated with 27.5 GeV positrons and 820 GeV protons. The measured reaction (1) is distinguished topologically by selecting events with one scattered positron and only four charged particles, two positive and two negative.

[1] The E665 experiment at the Tevatron has recently presented preliminary results, dominantly at low Q^2, expected to provide very useful information in this field [5].

[2] The $I = 1$ ϱ mesons other than $\varrho(770)$ are hereafter referred to as ϱ'.

Comparison is made with the production of $\varrho(770) \to \pi^+\pi^-$ in the reaction

$$ep \to e\pi^+\pi^- p \tag{2}$$

in the same Q^2 and W region, for which the final state is required to contain only two oppositely charged particles in addition to the scattered positron [11].

In all that follows, reference is made to elements of the H1 detector about which more details may be found in [12]. The cartesian coordinate system used takes the z axis to be along the outgoing proton, or forward, direction.

Events of reactions (1) and (2) were selected from the sample of ep large Q^2 events used to determine the proton structure function F_2 [13]. The trigger required a localised deposition of energy greater than 8 GeV in the backward electromagnetic calorimeter (BEMC). The scattered positron was detected in the BEMC as an electromagnetic cluster of energy greater than 12 GeV, associated with a hit in the backward proportional chamber (BPC) situated immediately in front of it. The final state hadrons were required to be detected in the central tracking detector, which consists of two coaxial cylindrical drift chambers CJC1 and CJC2. Their momentum component transverse to the beam direction had to exceed 100 MeV/c, as determined from the curvature of the tracks in the uniform 1.15 T magnetic field generated by the superconducting solenoid surrounding CJC1, CJC2 and the liquid argon calorimeter. This calorimeter covers the range $4 < \theta < 153^{\mathrm{o}}$ in polar angle. For both samples of events, the energy in the calorimeter, other than that associated with the tracks, was required to be below 0.1 GeV after application of a special algorithm for noise suppression. To reduce background from beam-gas interactions, an event vertex had to be reconstructed using the tracks and lie within 30 cm of the nominal interaction point in z.

Using a now standard and well evaluated technique [11, 14, 15], the forward components of the H1 detector ($\eta < 7.5$ [3]) were used to select a sample of elastic candidate events, in which the recoiling system is a proton. In the case of higher mass excitation of the target,

$$ep \to e\pi^+\pi^-\pi^+\pi^- Y \tag{3}$$

$$ep \to e\pi^+\pi^- Y \tag{4}$$

particles from the decay of the baryon recoil system Y are efficiently detected in the proton remnant tagger (PRT), the forward muon system (FM) and the forward part of the liquid argon calorimeter, either directly, or indirectly from secondary interactions which they make with the beam pipe and adjunct material. In the present selection, no hits were required in the PRT and no more than one pair of hits in the first three layers of FM. The resulting samples then correspond to events with $|t| \lesssim 1$ GeV^2 (t is the square of the four-momentum transfer at the proton vertex) and for which the mass of the system Y is less than ≈ 1.6 GeV/c^2 [16]. The remaining background from proton dissociation events in the elastic samples (1) and (2) is taken here to be $9 \pm 6\%$, as estimated in [11] using the Monte Carlo simulation [17], cross checked with the data.

Finally, to reduce the effects of initial state QED radiation, the $E - p_z$ of each event was required to be in the range $45 < E - p_z < 65$ GeV.

[3]The pseudorapidity η is defined as $\eta = -\ln\tan\theta/2$, where θ is the polar angle with respect to the $+z$ direction.

3 Kinematic Reconstruction

The "double angle" method [18] was used to reconstruct the event kinematics [4]. Here the variables Q^2 and $y = Q^2/s \cdot x$ (s is the ep CM energy) are calculated from the polar angles θ and γ of the positron and meson system, both of which are well measured, using

$$Q^2 = 4E^2 \frac{\sin\gamma \cdot (1+\cos\theta)}{\sin\gamma + \sin\theta - \sin(\gamma+\theta)}$$
$$y = \frac{\sin\theta \cdot (1-\cos\gamma)}{\sin\gamma + \sin\theta - \sin(\gamma+\theta)}, \qquad (5)$$

where E is the incident positron energy.

The 4–momentum transfer squared t to the proton is determined from the transverse momenta of the positron $\vec{p}_{te}$ and of the meson system $\vec{p}_{tm}$ using

$$|t| = 4E_pE_p' \sin^2\theta_p'/2 \simeq (\vec{p}_{tp})^2 = (\vec{p}_{te} + \vec{p}_{tm})^2$$

where E_p, E_p' are the initial and final proton energies, and θ_p' is the final proton polar angle. The momentum of the meson system is determined from the reconstructed pion tracks, and that of the scattered positron from Q^2 and y (5) rather from the less accurate direct measurement in the BEMC.

In addition to the event selections quoted above, the following kinematic cuts are imposed on the final samples:

$$Q^2 > 4 \text{ GeV}^2$$
$$40 < W < 140 \text{ GeV}^2$$
$$|t| < 0.6 \text{ GeV}^2. \qquad (6)$$

4 Acceptance Corrections

Corrections to the event samples of reactions (1) and (2) were determined by Monte Carlo event simulation [17].

The events were generated following a recipe inspired by the vector dominance model [19], which allowed the dependence of the production cross section on Q^2, W and t to be varied. For the study of reaction (1), the ϱ' resonance decay was generated as a two body decay into a ϱ meson and a $\pi^+\pi^-$ system, which in turn is made to decay uniformly in the available phase space.

The generated events were passed through a detailed simulation of the H1 detector, and subjected to the same reconstruction, trigger and selection procedures as the data samples.

After comparison with the observed distributions in the data, the acceptance was found to be 42% for ϱ' production with $\pi^+\pi^-\pi^+\pi^-$ invariant mass in the range $1.2 - 1.7$ GeV/c^2 and 59% for ϱ production in the $\pi^+\pi^-$ mass range $0.6 - 1.0$ GeV/c^2 for the cuts (6). A large part of the acceptance corrections comes from the geometric acceptance for positron identification in the BEMC–BPC.

[4] Particle masses are always taken to be negligible.

5 Nature of the $\pi^+\pi^-\pi^+\pi^-$ system

5.1 Mass Spectra

Figure 1 shows the $m_{4\pi}$ distribution for the events of reaction (1) for the kinematic region (6). A substantial enhancement is visible, peaking at $m_{4\pi} \sim 1.55$ GeV/c^2. This feature contrasts with the measurement at low W and Q^2 which is reported in [6] and in which no such strong enhancement is to be seen (see discussion in section 6.3 below).

Figure 2 shows the $m_{2\pi}$ mass spectra for the unlike sign $\pi^+\pi^-$ combinations (4 combinations per event) and for the like sign $\pi^\pm\pi^\pm$ combinations (2 combinations per event), for events of reaction (1) with $1.2 < m_{4\pi} < 1.7$ GeV/c^2. The like sign spectrum is scaled up by a factor 2. An enhancement is observed in the unlike sign combinations in the ϱ mass region, over the distribution obtained from the like sign combinations. This provides clear evidence for $\varrho(770)$ production in the $\pi^+\pi^-\pi^+\pi^-$ system, the signal being compatible with the production of one ϱ meson per event.

Superimposed on the $m_{4\pi}$ mass spectrum in figure 1 is the result of a fit to a relativistic Breit–Wigner distribution with mass independent width, together with an incoherent non–resonant background. The background normalisation was left free, while the shape was obtained from the data, as a fifth degree polynomial fit of the $m_{4\pi}$ mass spectrum of events produced either with $t > 0.6$ GeV^2, or with additional energy deposited in the calorimeter. The χ^2 of the fit is 24/16 dof. The resulting mass $m_{\varrho'}$ and width $\Gamma_{\varrho'}$ of the resonant contribution are:

$$\begin{aligned} m_{\varrho'} &= 1.57 \pm 0.02\ (stat.) \pm 0.01\ (syst.)\ \mathrm{GeV/c^2} \\ \Gamma_{\varrho'} &= 0.18\ \ \pm 0.06\ (stat.) \pm 0.07\ (syst.)\ \mathrm{GeV/c^2}. \end{aligned} \tag{7}$$

The background shape was also left free, as a first, second or third degree polynomial distribution, and the limits of the fit region were also allowed to vary. The resonance mass is strongly constrained by the position of the peak, and is quite stable against any such variations. The width of the resonance is stable against changes in the background shape, but gets larger when the shape is left free and the fit region is extended to lower masses, where no events are observed in the signal. In the latter case, the background shape peaks at masses well above the resonance peak, which has little plausibility. The spread of results for the fitted mass and width is used to estimate the systematic uncertainties quoted in (7).

A total of 108 events are collected in the mass range $1.2 < m_{4\pi} < 1.7$ GeV/c^2 used for the studies below. Of these, 46 ± 10, i.e. $43 \pm 10\%$ are attributed to non–resonant background.

The $\pi^+\pi^-$ mass spectrum of the events of reaction 2 is shown in figure 3 for the kinematic region (6). A huge peak attributed to ϱ mesons is observed. It is interesting to note that there is no evidence for any enhancement of similar mass and width as (7) in the $\pi^+\pi^-$ mass distribution of this figure.

5.2 ϱ' Resonance

As will be shown below (see section 6.1), the peripheral nature of the production mechanism is similar to that for elastic ϱ electroproduction in the same kinematic range. If the 4π system is thus taken to be diffractively produced, all the above are consistent with the resonance interpretation of the peak in the $\pi^+\pi^-\pi^+\pi^-$ system as being dominantly $I^G J^P = 1^+1^-$ and therefore a candidate for a ϱ' state with a large decay branching ratio to $\varrho^0\pi^+\pi^-$.

The light quark spectroscopy of vector mesons with isospin $I = 1$ remains ambiguous despite decades of experiment [1]. The 1^3S_1 ($n^{2S+1}L_J$) $q\bar{q}$ ground state configuration of $\varrho(770)$ ($I = 1$) is not contentious. The assignments of $\varrho(1450)$ to 2^3S_1 $I = 1$ and of $\varrho(1700)$ to 1^3D_1 $I = 1$, which are proposed in [1], are controversial. Much of this controversy arises because of ambiguities due to the complications of disentangling resonant contributions overlapping in mass spectra and interfering because of their large decay widths and common quantum numbers. The plausible ϱ' assignments above are based on the results of coupled channel analyses of data which include production of $\pi^+\pi^-$, $\pi^+\pi^-\pi^+\pi^-$, $\omega\pi^0$ and $\eta\varrho^0$ in e^+e^- annihilation [21, 22] and τ lepton decay [23].

5.3 Two Resonance Fit

It is clear that the identification of the enhancement in figure 1 in terms of the production and decay of one of the $\varrho(1450)$ or $\varrho(1700)$ meson is dubious given the values (7) of the resonance mass and width. Intuition, based on the radial properties of non-relativistic $q\bar{q}$ S and D wave functions, suggests that the production at high Q^2 of a ${}^3D_1$ vector meson is likely to be suppressed relative to that of a ${}^3S_1$ state. This is manifestly the case for the $c\bar{c}$ $\psi(2S)/\psi(3770)$ system. For light quark systems, a more realistic approach is probably to assume that there is substantial mixing between these S and D wave functions. Therefore the possibility should be considered that the single enhancement which is observed may be due to the production of two overlapping and interfering resonances.

The results of such a fit are shown in figure 4. The mass spectrum is fitted to a line shape of the form

$$|BW(m_{\varrho(1450)}, \Gamma_{\varrho(1450)}) + \alpha e^{i\beta} \cdot BW(m_{\varrho(1700)}, \Gamma_{\varrho(1700)})|^2$$

where $BW(m_\varrho, \Gamma_\varrho)$ are relativistic Breit–Wigner amplitudes with mass independent widths. The relative amplitude of $\varrho(1700)$ with respect to $\varrho(1450)$ is given by the parameter α and the phase β. The masses and widths of the $\varrho(1450)$ and $\varrho(1700)$ are taken from [1], the free parameters being α, β and the background normalisation. The fit for $1.0 < m_{4\pi} < 3.0$ GeV/c^2 gives

$$\alpha = 1.0 \pm 0.3 \qquad \beta = 3.1 \pm 0.9. \tag{8}$$

The χ^2 of the fit is nearly as good as for one resonance fit with free parameters: 27/16 dof. instead of 24/16 dof; given the uncertainties on the background shape, this difference is not considered significant. The preferred value of the phase is thus close to 180°, with nearly equal contributions of the two resonances. If a phase of 90° is imposed, the χ^2 is unchanged (27/17 dof.). However, if the two resonances are imposed to be in phase ($\beta = 0°$), the χ^2 is significantly worse: 35/17 dof.

The mass spectrum is thus well reproduced provided there is constructive interference in the mass region between the resonances ($\beta \sim 180^o$), suggesting that the interpretation of the ϱ' spectrum in [1] based on the coupled channel analyses of [21, 22, 23] is tenable in high Q^2 electroproduction, if both states have significant decay branching ratios to $\pi^+\pi^-\pi^+\pi^-$.

6 ϱ' Production Characteristics

6.1 t Dependence

For the study of the t distribution, the BPC hit associated with the positron was requested to lie outside a square of 32×32 cm^2 around the beam pipe, in order to provide precise association with the cluster in the case of showering of the electron before reaching the BPC. An additional cut of $Q^2 > 8$ GeV^2 was thus also imposed to the selected data. The t distribution of the thus selected events in the mass range $1.2 < m_{4\pi} < 1.7$ GeV/c^2 is shown in figure 5. The resonance production is clearly peripheral.

The t distribution is fitted in the region $|t| < 0.6$ GeV^2, as the sum of three exponentially falling contributions of the form $\mathrm{d}N/\mathrm{d}t = e^{bt}$: a contribution for elastic resonance production, with unknown b slope, a contribution for resonance production with proton dissociation, with a slope $b = 2.5 \pm 1.0$ GeV^{-2}, compatible with that measured for ϱ mesons [20] (no dependence of the slope on the proton excitation mass is assumed), and a non–resonant contribution with slope $b = 0.4 \pm 0.2$ GeV^{-2}, as obtained from a fit of the t distribution of the events containing in the liquid argon calorimeter a total energy over noise larger than 0.1 GeV. The relative contributions of these backgrounds to the number of events in the selected mass range were fixed at the values $9 \pm 6\%$ and $43 \pm 10\%$ quoted above.

The resulting slope for the elastic resonance production is found to be

$$b = 5.5 \pm 1.9 \text{ (stat.)} \pm 0.5 \text{ (syst.) GeV}^{-2}. \tag{9}$$

The systematic error includes the effects of varying the amount of each background and its b slope within errors, and those of changing the details of the fitting procedure. The background of events due to proton dissociation has little influence on this value.

It is an interesting cross check of the background extraction dicussed in section 5.2, that the fit of the t distribution up to $|t| = 6$ GeV^2 with two exponentials of slopes respectively 5.5 and 0.4 GeV^{-2} leads to an estimate of 47% background for $|t| < 0.6$ GeV^2, in agreement with the $43 \pm 10\%$ estimate from the mass spectrum.

For $\varrho(770)$ production, a similar parametrisation yields $b = 7.0 \pm 0.8 \pm 0.6$ GeV^{-2} [11].

6.2 Ratio of $\varrho'(\rightarrow \pi^+\pi^-\pi^+\pi^-)$ to ϱ Production Cross Sections

The ratio of the ϱ' to ϱ elastic production cross sections are given below in two forms. First, for the signal in the mass range $1.2 < m_{4\pi} < 1.7$ GeV/c^2, with no attempt to correct for the tail of the ϱ' resonance(s) (in this case, also the ϱ cross section is quoted only for the selected mass range $0.6 < m_{2\pi} < 1.0$ GeV/c^2). Second, as a corrected cross section when the enhancement in the 4π mass spectrum is considered as a single resonance, with parameters (7); in this case, the ϱ cross section is given for the mass range up to 1.5 GeV/c^2, in view of the uncertainty on the treatment of the large mass tail (see [11]). Since the $\varrho' \to \pi^+\pi^-\pi^+\pi^-$ branching ratio is unknown, the cross section ratio is given for this channel only. All results below are quoted for the kinematic range $Q^2 > 4$ GeV^2, $40 < W < 140$ GeV/c^2.

The selection criteria are the same for the two samples, except for the number of charged particles and the mass range. In particular, the algorithms for track–cluster association and for noise suppression were the same for the two samples. The similarity of the b slopes allows the same cut in $|t|$ at 0.6 GeV^2.

The raw numbers of selected events for the ϱ' and ϱ contributions are, respectively, 108 and 301. The cross section ratio was computed from these numbers of events, corrected for the contributions of the non–resonant backgrounds (the proton dissociation backgrounds were assumed to be the same), and for efficiencies and acceptances. These were estimated using the same Monte Carlo reconstruction program

The largest uncertainties in the ratio come from the non–resonant background subtraction in the ϱ' sample (20%) and in the ϱ sample (6%). The uncertainties on the ϱ' and the ϱ acceptances are estimated to lead to uncertainties in the ratio below 5%. This was obtained by varying the parameters of the track–cluster association, by imposing more stringent criteria for track selection (p_t cut, angular selection), and by changing the energy allowed in the calorimeter after application of the noise suppression algorithm. All these errors partly cancel in the ratio but not completely, because of the different charged particle multiplicities. Other small uncertainties were also included in the systematic errors below (corrections for the t cuts due to the uncertainties in the b slope, mass resolution, limited Monte Carlo statistics).

The ϱ' / ϱ cross section ratio for the limited mass ranges is

$$\frac{\sigma(ep \to e\varrho'(\pi^+\pi^-\pi^+\pi^-)p; 1.2 < m_{4\pi} < 1.7)}{\sigma(ep \to e\varrho p; 0.6 < m_{2\pi} < 1.0)} = 0.33 \pm 0.06 \text{ (stat.)} \pm 0.08 \text{ (syst.)}. \quad (10)$$

The ratio for the one ϱ' resonance assumption with parameters (7) and for $m_{2\pi} < 1.5$ GeV/c^2 is

$$R_{\varrho'/\varrho} = \frac{\sigma(ep \to e\varrho'(\pi^+\pi^-\pi^+\pi^-)p)}{\sigma(ep \to e\varrho p; m_{2\pi} < 1.5)} = 0.36 \pm 0.07 \text{ (stat.)} \pm 0.11 \text{ (syst.)}. \quad (11)$$

The latter cross section ratio is also given in Table 1, in two bins in Q^2 and in two bins in W. The assumption is made that the relative contribution of non–resonant background is independent of Q^2 and W. This assumption could not be cross checked with the data, because of statistical limitations. Even taking into account that the systematic uncertainties are largely correlated, no evidence is found for a Q^2 or W dependence of the ratio.

6.3 Discussion

The production and decay in the $\pi^+\pi^-\pi^+\pi^-$ channel of $\varrho'(1600)$ meson have been studied by a small number of photo- and leptoproduction experiments, mostly at low energy.

$40 < W < 140$ GeV/c^2 $\langle W \rangle \approx 85$ GeV/c^2	
$4 < Q^2 < 9$ GeV^2 $\langle Q^2 \rangle \approx 7$ GeV^2	$9 < Q^2 < 50$ GeV^2 $\langle Q^2 \rangle \approx 15$ GeV^2
$R_{\varrho'/\varrho} = 0.35 \pm 0.09 \pm 0.11$	$R_{\varrho'/\varrho} = 0.38 \pm 0.10 \pm 0.11$
$4 < Q^2 < 50$ GeV^2 $\langle Q^2 \rangle \approx 11$ GeV^2	
$40 < W < 85$ GeV/c^2 $\langle W \rangle \approx 62$ GeV/c^2	$85 < W < 140$ GeV/c^2 $\langle W \rangle \approx 110$ GeV/c^2
$R_{\varrho'/\varrho} = 0.35 \pm 0.09 \pm 0.10$	$R_{\varrho'/\varrho} = 0.38 \pm 0.10 \pm 0.11$

Table 1: Values in different Q^2 and W domains of the cross section ratio $R_{\varrho'/\varrho}$ ($\varrho' \rightarrow \pi^+\pi^-\pi^+\pi^-$). The ϱ' signal is corrected for acceptance as one resonance with parameters (7); the ϱ signal is corrected for acceptance for $m_{2\pi} < 1.5$ GeV/c^2.

Two photoproduction experiments have reported results at high energy. The first (Atiya et al. [2]) studied ϱ' production on a C target exposed to 50 GeV photons at Fermilab. Only a statistical error is quoted for ϱ' production. The $R_{\varrho'/\varrho}$ ratio was computed here using for the ϱ mesons a cross section from a compilation [24]. The second (Aston et al. [3]) uses the OMEGA spectrometer at CERN, exposed to photons with energy $20 - 70$ GeV. The $R_{\varrho'/\varrho}$ ratio is not directly measured, but can be computed as $0.07 \pm 0.03 \pm 0.03$ using the cross section for ϱ meson production in the same experiment [25].

In leptoproduction, only two experiments have reported results. At low energy (11.5 GeV electron beam at Cornell) and $\langle Q^2 \rangle \approx 1$ GeV^2, Killian et al. [6] quote estimates for the productions of ϱ' and ϱ mesons, without errors, from which the ratio can be evaluated to be of the order of 0.13. With the Fermilab muon beam at 100 and 150 GeV i.e. for $\langle W \rangle \approx 11$ and 14 GeV/c^2 and $\langle Q^2 \rangle \approx 0.4$ GeV^2, the CHIO Collaboration (Shambroom et al. [4]) measures (uncorrected) $R_{\varrho'/\varrho}$ ratios of 0.06 and 0.13, with statistical errors of the order of 20%.

These results are presented in figure 6, together with the results of the present analysis. The increase of the ratio with Q^2 is striking, in spite of the large uncertainties affecting the data, and in particular the unknown total errors and background contributions affecting the fixed target leptoproduction results.

This increase is strong enough to be suggestive of the QCD inspired phenomena discussed in [7, 8, 9, 10]. In this approach, the cross section for elastic vector meson production is given by the convolution of three factors: the probability for the virtual photon to emit, at a large distance from the target, a $q\bar{q}$ pair of given lateral dimension, the colour dipole–proton cross section, and the transverse size of the final state vector meson. At small Q^2, large distances (small k_t) in the $q\bar{q}$ pair and non–perturbative amplitudes dominate, whereas at higher Q^2, small distance $q\bar{q}$ pairs play an increasing role, with a resolution which allows the scanning of the final state meson wave functions.

In the presence of a node in the vector meson wave, low Q^2 interactions, lacking resolution and integrating over all distances, are expected to reveal cancellation effects. If the observed enhancement corresponds to a state presenting such a node, e.g. if it is an excited $2S$ resonance [5], the small cross section measured in photoproduction and low Q^2 leptoproduction could be explained. At very large Q^2, in contrast, with dominating small transverse sizes, the cancellation effects would not take place, and cross sections of the same order of magnitude would be expected for the ϱ' and the ϱ.

In the HERA range, indications exist of an interplay for light vector meson production between perturbative and non–perturbative effects, leading to a transition regime [11]. The qualitative pictures above have thus to be modulated accordingly. A ratio $R_{\varrho'/\varrho}$ in the range $0.3 - 0.4$ is predicted [9, 10]. The present results are thus an indication that this promising way of studying the nature of the pomeron could be explored at HERA.

7 Conclusion

A significant enhancement has been observed in the $\pi^+\pi^-\pi^+\pi^-$ mass spectrum of the elastic production of four charged pions in the kinematic domain $4 < Q^2 \lesssim 50$ GeV^2, $40 < W < 140$ GeV/c^2.

The interpretation of this as a single $I^G J^P = 1^+1^-$ ϱ' resonance with mass 1.57 ± 0.02 GeV/c^2 and width 0.18 ± 0.09 GeV/c^2 with a large decay branching ratio to $\varrho^0\pi^+\pi^-$, is consistent with all observations made here concerning both production and decay of the 4π system. The hypothesis of the coherent production of two ϱ' resonances, $\varrho(1450)$ and $\varrho(1700)$, for which tenuous evidence exists from e^+e^- annihilation and τ lepton decay, is also consistent with the data, offering some hope that a consistent picture will emerge of the ϱ' resonances.

The resonant systems are produced in a peripheral process. The t distribution of the events is parameterised as exponentially falling, with a slope $b = 5.5 \pm 1.9 \pm 0.5$ GeV^{-2}.

A major result of the present study is the measurement of the ratio of the elastic production cross sections for ϱ' and ϱ mesons at high Q^2 and high W. This ratio is found to be $R_{\varrho'/\varrho} = 0.36 \pm 0.07 \pm 0.11$, integrated over the kinematic domain accessed here. This value is significantly higher that those measured in photo– or leptoproduction with $Q^2 \lesssim 1$ GeV^2. Inside the present data however, no significant Q^2 dependence of this ratio is observed from $\langle Q^2 \rangle = 7$ GeV^2 to $\langle Q^2 \rangle = 15$ GeV^2, nor from $\langle W \rangle = 60$ GeV/c^2 to $\langle W \rangle = 110$ GeV/c^2, making the assumption that the relative contribution of the non–resonant background is independent of Q^2 and W. A significant increase of $R_{\varrho'/\varrho}$ from $Q^2 \simeq 0$ to the present Q^2 range is predicted in QCD approaches based on the colour dipole phenomenology.

The present results are thus an encouraging indication that the study of the elastic production of vector mesons in excited states at HERA might shed additional light on the nature of diffraction and the structure of the pomeron.

[5] In the hypothesis that the signal is due to two interfering resonances, more subtle effects might take place.

8 Acknowledgments

We are grateful to the HERA machine group whose outstanding efforts have made and continue to make this experiment possible. We thank the engineers and technicians for their work in constructing and now maintaining the H1 detector, our funding agencies for financial support, the DESY technical staff for continual assistance, and the DESY directorate for the hospitality which they extend to the non–DESY members of the collaboration. We also acknowledge gratefully interesting discussions with B. Kopeliovich and M. Strikman.

References

[1] Particle Data Group: L. Montanet et al., Phys. Rev. **D54** (1996), *Meson Particle Listings*, p.373, and references therein.

[2] M.S. Atiya et al., Phys. Rev. Lett. **43** (1979) 1691.

[3] D. Aston et al., Nucl. Phys. **B189** (1981) 15.

[4] CHIO Collaboration, W.D. Shambroom et al., Phys. Rev. **D26** (1982) 1.

[5] E665 Collaboration, C. Salgado, CEBAF Workshop on Colour Transparency (1995).

[6] T. J. Killian et al., Phys. Rev. **D21** (1980) 3005.

[7] B.Z. Kopeliovich and B.G. Zakharov, Phys. Rev. **D44** (1991) 3466.

[8] B.Z. Kopeliovich et al., Phys. Lett. **B309** (1993) 179.

[9] L. Frankfurt, W. Koepf and M. Strikman, *Hard diffractive electroproduction of vector mesons in QCD,* preprint TAUP-2290-95, hep-ph/9509311 (1995).

[10] J. Nemchik et al., *Colour dipole phenomenology of diffractive electroproduction of light vector mesons at HERA*, preprint DFTT 71/95, KFA-IKP(TH)-24-95, hep-ph/9605231 (1996).

[11] H1 Collaboration, S. Aid et al., Nucl. Phys. **B468** (1996) 3, and paper pa02–066 submitted to this conference.

[12] H1 Collaboration, I. Abt et al., DESY internal report H1–96–01 (1996);
H1 Collaboration, I. Abt et al., DESY preprint DESY 93–103 (1993);
H1 Calorimeter Group, B. Andrieu et al., Nucl. Inst. Meth. **A336** (1993) 460, ibid. **A336** (1993) 499, ibid. **A350** (1994) 57.

[13] H1 Collaboration, S. Aid et al., Nucl. Phys. **B470** (1996) 3.

[14] H1 Collaboration, T. Ahmed et al., Phys. Lett. **B348** (1995) 681.

[15] H1 Collaboration, S. Aid et al., *Elastic and Inelastic Photoproduction of J/ψ Mesons at HERA*, preprint DESY-96-37, subm. to *Nucl. Phys.*

[16] H1 Collaboration, S. Aid et al., *A Measurement and QCD Analysis of the Diffractive Structure Function* $F_2^{D(3)}$, paper pa02-061 submitted to this conference.

[17] DIFFVM program, see: B. List, *Diploma Thesis*, Techn. Univ. Berlin, unpubl. (1993).

[18] S. Bentvelsen, J. Engelen and P. Kooijman, *Reconstruction of* (x, Q^2) *and Extraction of Structure Functions in Neutral Current Scattering at HERA*, in Proc. of the Workshop on Physics at HERA, ed. W. Buchmueller and G. Ingelman, Hamburg 1992 Vol. 1, p. 23;
K. C. Hoeger, *Measurement of* x, y, Q^2 *in Neutral Current Events*, ibid., p. 43.

[19] T.H. Bauer et al., Rev. Mod. Phys. **50** (1978) 261, and references therein.

[20] H1 Collaboration, S. Aid et al., *Electroproduction of* ϱ *Mesons with Proton Diffractive Dissociation at* $Q^2 > 7$ GeV^2 *at HERA*, paper pa02-065 submitted to this conference.

[21] A. Donnachie and H. Mirzaie, Zeit. Phys. **C33** (1987) 407 and references therein.

[22] A. Donnachie and A. B. Clegg, Zeit. Phys. **C34** (1987) 257 and references therein.

[23] A. B. Clegg and A. Donnachie, Zeit. Phys. **C40** (1988) 313 and references therein.

[24] H1 Collaboration, S. Aid et al., Nucl. Phys. **B463** (1996) 3.

[25] D. Aston et al., Nucl. Phys. **B209** (1982) 56.

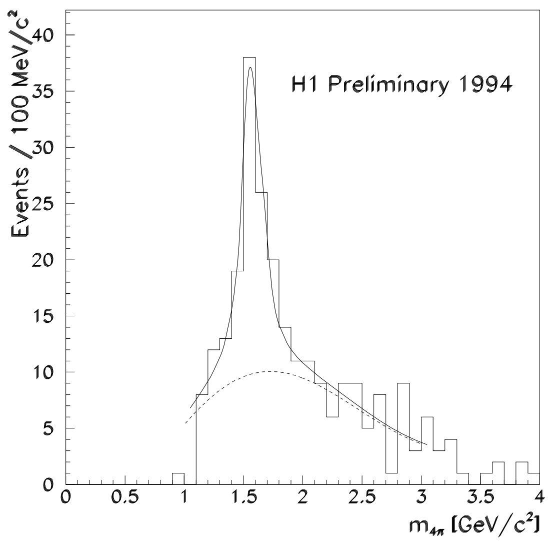

Figure 1: Distribution of the $m_{4\pi}$ invariant mass for the selected events of reaction $ep \rightarrow e\pi^+\pi^-\pi^+\pi^-p$, showing an enhancement at $\sim$ 1.55 GeV/c^2. The superimposed curve describes the result of a fit to a single resonance with free mass and width, over a background of imposed shape, represented by the dotted curve (see text).

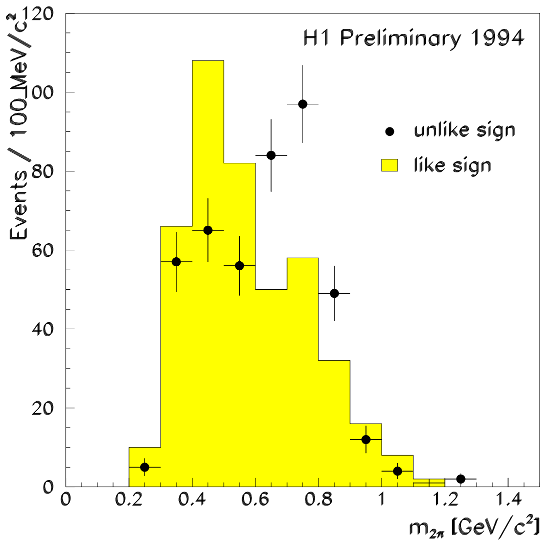

Figure 2: Distribution of the $m_{2\pi}$ invariant mass for the selected events of reaction $ep \rightarrow e\pi^+\pi^-\pi^+\pi^-p$. The points correspond to the unlike sign $\pi^+\pi^-$ combinations and the shaded histogram to the like sign $\pi^\pm\pi^\pm$ combinations, scaled up by a factor 2. A signal for the ϱ resonance is observed in the unlike sign distribution.

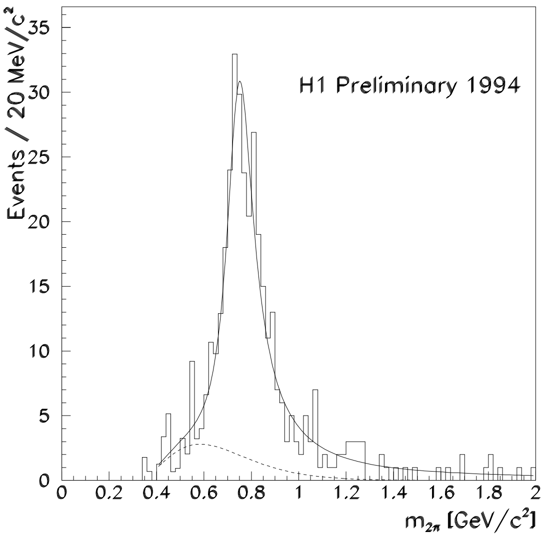

Figure 3: Distribution of the $m_{2\pi}$ invariant mass for the selected events of reaction $ep \to e\pi^+\pi^-p$, showing a large contribution at the ϱ resonance mass. The superimposed curve describes the result of a fit to a the ϱ resonance, over a phase space like background, represented by the dotted curve (see [11]).

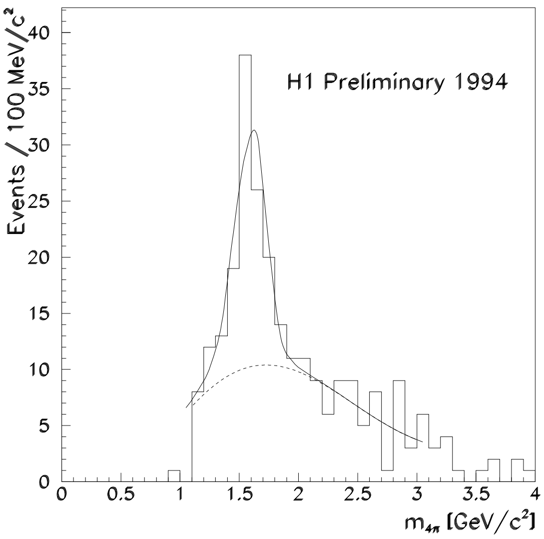

Figure 4: Distribution of the $m_{4\pi}$ invariant mass for the selected events of reaction $ep \to e\pi^+\pi^-\pi^+\pi^-p$. The superimposed curve describes the result of a fit to two resonances with mass and width fixed at the PDG values [1] for $\varrho(1450)$ and $\varrho(1700)$ with free normalisation and phase, over a background of imposed shape, represented by the dotted curve (see text).

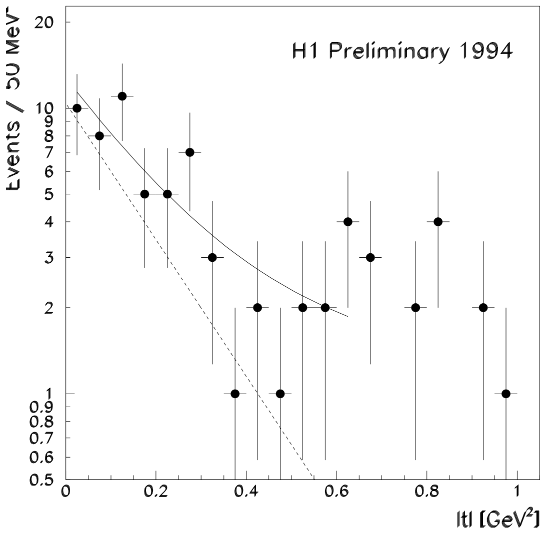

Figure 5: Distribution of t, the four momentum transfer squared to the proton, for the selected events of reaction $ep \to e\pi^+\pi^-\pi^+\pi^- p$. The full curve represents a fit to the sum of three exponential distributions described in the text. The dotted curve represents the fitted contribution for elastic ϱ' production.

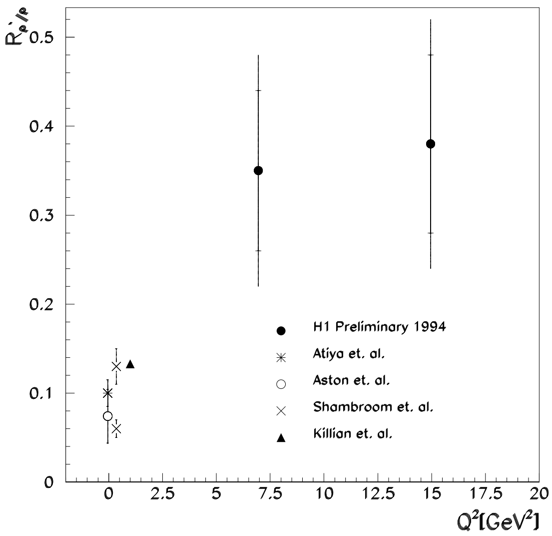

Figure 6: Ratio $R_{\varrho'/\varrho}$ of the cross sections for $\varrho' \to \pi^+\pi^-\pi^+\pi^-$ and ϱ meson elastic production as a function of Q^2, for several experiments. The inner error bars describe the statistical errors and the full error bars the statistical and systematic errors combined in quadrature, when they are available; when they are not, large normalisation uncertainties presumably affect the ratios.